Application of dynamic subgrid-scale concepts from large-eddy simulation to modeling landscape evolution

Paola Passalacqua,[1,2,3] Fernando Porté-Agel,[1,2,3] Efi Foufoula-Georgiou,[1,2,3] and Chris Paola[1,2,4]

[1]   Landscapes share important similarities with turbulence: both systems exhibit scale invariance (self-similarity) over a wide range of scales, and their behavior can be described using comparable dynamic equations. In particular, modified versions of the Kardar-Parisi-Zhang (KPZ) equation (a low-dimensional analog to the Navier-Stokes equations) have been shown to capture important features of landscape evolution. This suggests that modeling techniques developed for turbulence may also be adapted to landscape simulations. Using a "toy" landscape evolution model based on a modified 2-D KPZ equation, we find that the simulated landscape evolution shows a clear dependence on grid resolution. In particular, mean longitudinal profiles of elevation at steady state and bulk erosion rates both have an undesirable dependence on grid resolution because the erosion rate increases with resolution as increasingly small channels are resolved. We propose a new subgrid-scale parameterization to account for the scale dependence of the sediment fluxes. Our approach is inspired by the dynamic procedure used in large-eddy simulation of turbulent flows. The erosion coefficient, assumed exactly known at the finest resolution, is multiplied by a scale dependence coefficient, which is computed dynamically at different time steps on the basis of the dynamics of the resolved scales. This is achieved by taking advantage of the self-similarity that characterizes landscapes over a wide range of scales. The simulated landscapes obtained with the new model show very little dependence on grid resolution.

1.   Introduction

[2]   The fascinating self organized spatial patterns of natural landscapes have long attracted the attention of researchers. The most obvious and widespread of these patterns are the tributary channel networks generally characteristic of erosional landscapes. Building on earlier landscape models such as those of *Culling* [1960, 1963], which used a diffusion model of slope erosion, the 1990s saw a renaissance of landscape modeling [e.g., *Willgoose et al.*, 1991a, 1991b; *Chase*, 1992; *Rinaldo et al.*, 1992; *Howard*, 1994; *Rodriguez-Iturbe et al.*, 1994; *Rodriguez-Iturbe and Rinaldo*, 1997; *Smith et al.*, 1997a, 1997b; *Tucker et al.*, 2001]. In general, these models have focused on reproducing "whole-system" properties of the landscape such as fractal dimensions, network topology, and spatial statistics (e.g., slope distributions, slope-area relations). Landscape evolution models have also been coupled to tectonic models to simulate the evolution of mountain belts on long time-scales [*Kooi and Beaumont*, 1994; *Tucker and Slingerland*, 1994; *Koons*, 1995]. Comprehensive reviews on landscape evolution modeling approaches are given on *Dietrich et al.* [2003], *Peckham* [2003], and *Willgoose* [2005].

[3]   A fundamental problem arises in numerical modeling of systems whose dynamics spans a wide range of scales: selection of a computational grid (usually dictated by the size of the domain over which a solution is sought and the smallest grid that can be afforded computationally) leaves out scales whose dynamics are not explicitly resolved. Yet, it is known that even if the interest is not in resolving the smallest scales, their effect on the dynamics of the larger scales (due to nonlinearities) is considerable. Thus ignoring the subgrid scales compromises the accuracy of the solution at the resolved scales and also makes the numerical simulation resolution-dependent. This problem presents itself in numerical modeling of many natural processes which exhibit multiscale variability, including flow and transport in porous media, atmospheric modeling from cloud resolving models to mesoscale to global circulation models, land-atmosphere interactions, atmospheric turbulence and, foremost, modeling of turbulent flows. Several methodologies have been proposed to address this problem and these include derivation of "effective" parameters in coarse grained equations [e.g., *Bear*, 1988; *Bou-Zeid et al.*, 2004], statistical downscaling [e.g., *Harris and Foufoula-*

---

[1]St. Anthony Falls Laboratory, Minneapolis, Minnesota, USA.
[2]National Center for Earth-Surface Dynamics (NCED), Minneapolis, Minnesota, USA.
[3]Department of Civil Engineering, University of Minnesota–Twin Cities, Minneapolis, Minnesota, USA.
[4]Department of Geology and Geophysics, University of Minnesota–Twin Cities, Minneapolis, Minnesota, USA.

Georgiou, 2001], and analytical derivation of closure terms [e.g., *Meneveau and Katz*, 2000; *Sagaut*, 2002], among others.

[4] The field in which subgrid-scale parameterizations have been the most advanced is that of turbulence, where direct numerical simulation (DNS), i.e., numerical solution of the Navier-Stokes equations using a resolution as small as the dissipation (Kolmogorov) scale, is only feasible for relatively low Reynolds number flows. A technique that has become popular to simulate higher Reynolds number turbulent flows is large-eddy simulation (LES), which consists of solving the spatially filtered Navier-Stokes equations, using a spatial filter of size equal to or slightly larger than the grid size. This filtering operation applied to the nonlinear advection terms leads to the so-called subgrid-scale fluxes, which represent the effect of the subgrid scales on the evolution of the resolved scales and need to be parameterized. As a result, LES explicitly resolves all scales of motion (eddies) larger than the grid scale, while the subgrid-scale fluxes are parameterized using a subgrid-scale model. Comprehensive reviews on LES and subgrid-scale modeling are given by *Meneveau and Katz* [2000], *Pope* [2000, 2004], and *Geurts* [2004]. A particularly interesting development in subgrid-scale modeling of turbulent flows is the so-called dynamic modeling approach [*Germano et al.*, 1991; *Moin et al.*, 1991; *Porté-Agel et al.*, 2000; *Porté-Agel*, 2004]. It takes advantage of the scale similarity of turbulence to optimize the value of the subgrid model coefficient(s) based on the dynamics of the resolved scales, thus not requiring any parameter tuning.

[5] In the case of landscape evolution, it is well known that landscapes present multiscale self-similar properties through a wide range of scales, from the system scale (typically $10^2 – 10^4$ km) down to the spacing of the smallest channels, which is typically on the order of $10 – 100$ m and below which diffusion processes dominate. As in high Reynolds number turbulence, numerical solution of the entire range of scales is usually impractical. Instead, landscape models are run at relatively coarse resolution, i.e., one solves the so-called coarse-grained transport equations (Figure 1). However, the accuracy of this methodology is unknown since channels smaller than the grid size are not taken into account. This suggests the possibility that the calculated erosion rates and landscape evolution are likely affected by the grid resolution. This was pointed out by *Stark and Stark* [2001] who developed a subgrid-scale parameterization based on a parameterization measure called channelization. *Rodriguez-Iturbe and Rinaldo* [1997] have shown the effect of "coarse graining" a specific landscape on the scaling relationships of elevation.

[6] Landscapes share important similarities with turbulence: both systems exhibit scale invariance (self-similarity) over a wide range of scales and their behavior can be described using comparable dynamic equations. This similarity can be seen, for example, in the behavior of power spectra: Turbulence velocity spectra exhibit a well-known $−5/3$ slope in the inertial subrange [*Kolmogorov*, 1961], representing the energy cascade from large scales to small scales. In the case of landscapes, power spectra of linear transects in topography also exhibit a log-log scaling range with slope of $−2$. Another parallel between the two systems is the existence of a lower limit on the size of the turbulent

structures (eddies): the Kolmogorov scale, the scale at which viscous effects dominate and the effective Reynolds number approaches unity. In landscapes, the analogous fine scale would be the spacing of the smallest channels, determined by the scale at which (diffusive) hillslope processes dominate [e.g., *Dietrich et al.*, 2003]. This analogy between the viscous length scale of turbulence and the hillslope scale in landscapes has also been discussed by others [e.g., *Peckham*, 1995]. Moreover, turbulence has been used as a metaphor for other complex systems such as earthquakes [*Kagan*, 1992] and stream braiding [*Paola*, 1996; *Paola et al.*, 1999].

[7] The purpose of this paper is to explore concepts of LES in the context of landscape evolution modeling. Using a minimum complexity model, used previously by several authors for landscape simulation [e.g., *Sornette and Zhang*, 1993; *Somfai and Sander*, 1997; *Banavar et al.*, 2001], we demonstrate its scale dependence and propose a dynamic subgrid-scale model to take into account the effect of subgrid-scale processes in a landscape evolution model.

[8] It is important to point out that the goal of this study is not to strictly apply the LES technique, as developed for turbulent flows, to landscape evolution simulations. There are some limitations to the direct extension of the LES technique to landscapes. Typical governing equations for landscape evolution, even though often similar in form to the Navier-Stokes equations (including nonlinear terms that generate fluctuations as well as diffusion terms), are not as well established for the description of the system at all scales. For example, the nonlinear erosion flux term is already a parameterization containing tuning coefficient(s). This makes it challenging to formally define the subgrid-scale erosion fluxes and to develop subgrid-scale models for them. Instead, our approach here consists of developing a tuning-free dynamic procedure, inspired from the dynamic modeling approach used in LES, to "optimize" the value of the erosion coefficient (in the nonlinear erosion flux term) using the scale dependence of the coefficient quantified from the smallest resolved scales in the simulations.

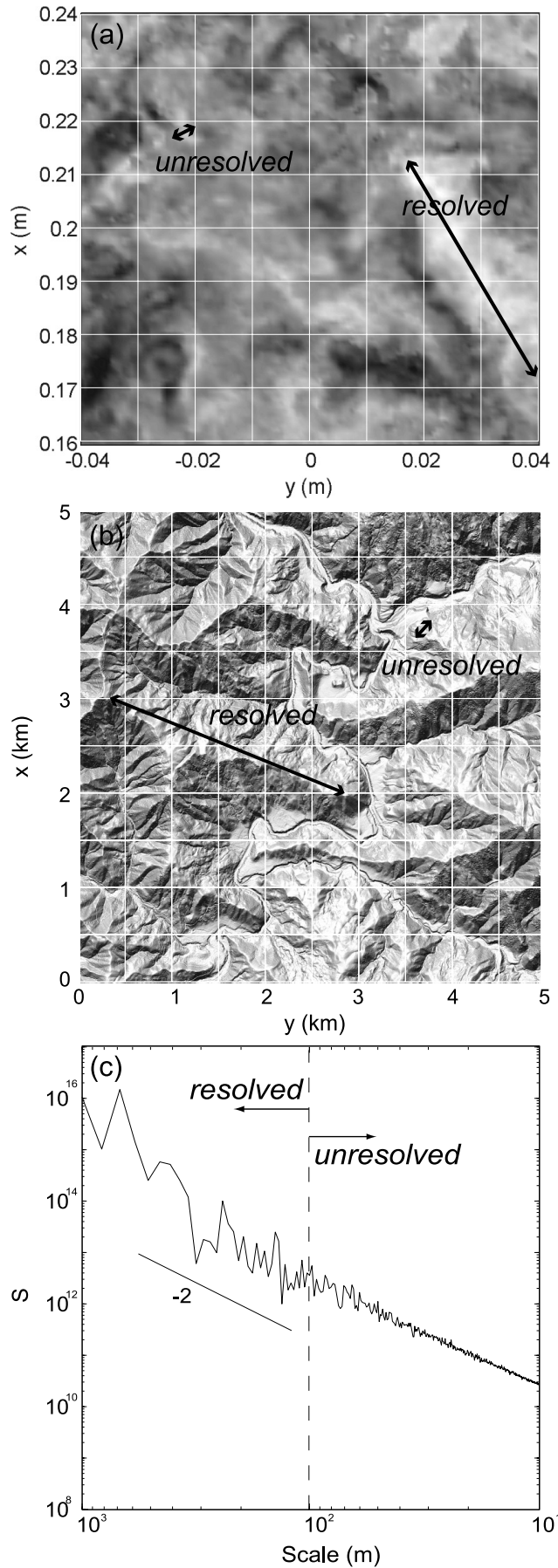## 2. Landscape Evolution Modeling and Effect of Grid Resolution

2.1. KPZ Model

[9] As discussed above, a number of different models have been proposed for landscape evolution. Here we use a modified version of the Kardar-Parisi-Zhang (KPZ) equation, originally used in the context of growth of atomic interfaces by ion deposition [*Kardar et al.*, 1986]. The KPZ equation as applied to modeling the evolution of land surface elevation h reads [*Sornette and Zhang*, 1993; *Somfai and Sander*, 1997; *Banavar et al.*, 2001]:

$$\frac{\partial h(\vec{x}, t)}{\partial t} = D\nabla^2 h + C|\nabla h|^2 + \eta(\vec{x}, t) \qquad (1)$$

The right hand side of equation (1) includes, from left to right, a diffusion term, where D is the diffusion coefficient, a nonlinear term, where C is a constant and ∇h is the slope, and a white noise term.

[10] It is important to note that, with a simple transformation of variables, the KPZ equation without noise

becomes the Burgers equation, a low-dimensional analog to the Navier-Stokes equations governing fluid flow and turbulence.

[11] The initial application of the KPZ equation to landscape evolution [*Sornette and Zhang*, 1993] shows the importance of the nonlinear terms in the evolution of surface topography and the associated drainage network. At a coarse grained scale, the effect of diffusion is often neglected [*Somfai and Sander*, 1997; *Banavar et al.*, 2001] since this mechanism is effective mainly at the small (subgrid) scales. Neglecting also the noise term, (1) has only the non linear term on the right hand side. Furthermore, taking into account that the evolution of the landscape is coupled with the water flux q acting on the surface, the constant C in front of the nonlinear term in (1) can be written as an erosion coefficient α times the water flux q [*Somfai and Sander*, 1997; *Banavar et al.*, 2001]. The governing equation then becomes:

$$\frac{\partial h}{\partial t} = -\alpha \cdot q \cdot |\nabla h|^2. \tag{2}$$

Under the assumption of uniform rainfall acting on the surface, the water flux at a given point is proportional to the area draining at that location. We have chosen a fairly simple landscape evolution model, best suited for bedrock landscape evolution modeling, which does not allow both erosion and deposition to occur. This choice has been motivated by the fact that a simple type of equation would maximize clarity in deriving the subgrid model. This work will be extended in the future to more comprehensive landscape evolution models.

[12] Notice that (2) is a special case of the general governing equation, widely used in landscape modeling [e.g., *Rodriguez-Iturbe and Rinaldo*, 1997]:

$$\frac{\partial h}{\partial t} = -\alpha \cdot A^m \cdot |\nabla h|^n, \tag{3}$$

with $\frac{m}{n} \approx 0.5$.

[13] The nature of the steady state reached by the system depends on the external conditions applied in the problem. If the boundary condition at the output is a fixed elevation, with constant rock uplift, the steady state is reached when the erosion rate balances the rock uplift rate over the whole system [*Hack*, 1960; *Adams*, 1980; *Howard*, 1994; *Somfai and Sander*, 1997; *Willett and Brandon*, 2002]. If the uplift

Figure 1. Schematic of the separation between resolved and subgrid scales in turbulence (Figure 1a) and landscapes (Figures 1b and 1c). (a) Gray scale rendering of the vertical velocity component measured in a turbulent boundary layer at the St. Anthony Falls Laboratory wind tunnel. (b) Bare-earth LIDAR shaded-relief image (1-m resolution) of a portion of the Angelo Coast Range Reserve, northern California, grid spacing of 500 m. (c) Fourier spectrum of the topography shown in Figure 1b, showing a −2 power law dependence of spectral power on wave number. Separation between resolved and unresolved scales is 100 m. In both turbulence and landscapes, only structures with length scales larger than the grid size are explicitly resolved.
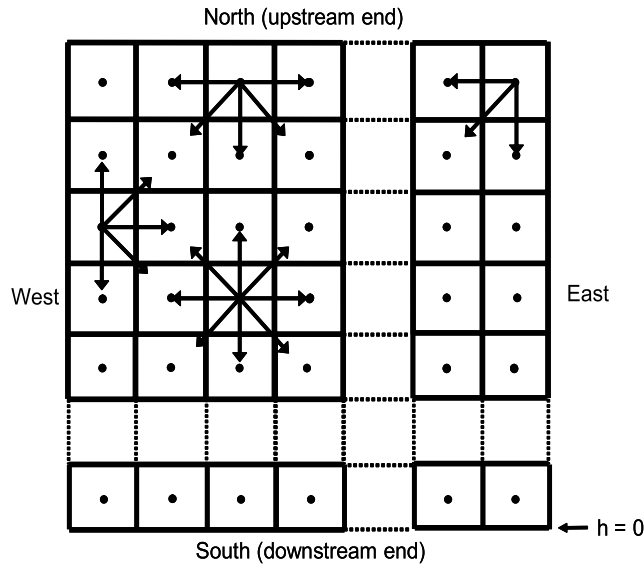
Figure 2. Boundary conditions and allowed flow directions. The output of the system is located at the downstream end of the field where the elevation is kept fixed at zero. At the upstream end the boundary condition is an infinite wall, so that no flow exits upstream of the field. At the east and west boundaries, the flow directions are likewise restricted to those inside the field. Thus the only allowed output is at the downstream end of the field.

rate is zero, the system reaches a steady state when there is no remaining material to erode [*Inaoka and Takayasu*, 1993].

[14] The river networks obtained with the modified KPZ equation have been shown to satisfy scaling laws characteristic of natural landscapes: the slope-area law, the power law of distribution of drainage area, and Horton's laws for branching ratio and length ratio [*Somfai and Sander*, 1997]. In addition to these laws, the simulations also yield realistic profiles for the average elevation along the mainstream direction [*Banavar et al.*, 2001].

2.2. Numerical Implementation

[15] The initial field is a sloping surface with a small noise, obtained using the following expression [*Somfai and Sander*, 1997]:

$$h(x, y, t = 0) = s_0 \cdot (y + dy \cdot rand(x, y)), \qquad (4)$$

where h is the elevation, s_0 represents the initial slope, y is the north-south coordinate, dy is the grid constant and *rand* is a uniform random number in the range [0,1]. This initial configuration prevents the formation of lakes.

[16] We study the evolution of the system at three different resolutions: the same field is divided into 256 × 256 grid cells, 128 × 128 grid cells and 64 × 64 grid cells. We focus initially on the simplest case (uniform rainfall, no groundwater, uniform and structureless substrate, no redeposition), applying the simplified erosion model discussed earlier (equation (2)) with the addition of a constant uplift u:

$$\frac{\partial h}{\partial t} = u - \alpha \cdot q \cdot |\nabla h|^2, \qquad (5)$$

Equation (5) represents an erosional model for an incisional process where the erosion rate depends linearly on water flux and nonlinearly on slope.

[17] Water is routed using the steepest descent rule. In every site the elevation is compared with the one of the eight surrounding neighbors and the water is assumed to follow the steepest path. Recently, *Pelletier* [2004] has shown that computing the slope using a multiple-direction algorithm eliminates an undesirable consequence of the steepest descent rule: evolution to a frozen steady state of the river network in which erosion exactly balances uplift at each point [*Hasbargen and Paola*, 2000, 2003]. Once the flow direction is computed in every site, the slope and the water flux can be computed and used to update the elevation via (5). Because of the assumption of a uniform rainfall and no loss of water, the water flux is given by the drainage area times the unit rainfall.

[18] The boundary conditions are: an infinite wall at the upstream end of the field (north boundary); an output boundary at fixed height equal zero located at the downstream end of the field (south boundary); on the lateral sides (east and west boundaries) the flow is forced to drain into the system. This condition could be easily changed to periodic boundary conditions [*Somfai and Sander*, 1997; *Banavar et al.*, 2001]. A sketch of the computational domain with the applied boundary conditions is shown in Figure 2.

[19] The simulations with the three resolutions are run independently until the systems reach steady state. The steady state is reached when the erosion rate is in equilibrium with the uplift. The simulated evolution of the landscape shows two different timescales: a freezing time, at which the river network reaches its final configuration but the elevation continues adjusting, and a relaxation time at which the system reaches its equilibrium profile and the surface stops evolving [*Sinclair and Ball*, 1996; *Banavar et al.*, 2001]. The time needed to freeze the system is usually smaller than the time needed to reach the final profile. It should be noted that a freezing time, and a corresponding frozen configuration of the system, can be defined as we have done only because the model allows for an (unrealistic) static steady state. Revised definitions would be needed for the more realistic dynamic-steady-state condition.

[20] The freezing time of the system is obtained by computing at every time step the number of unstable sites. An unstable site is defined as a point in the system where the flow direction changes in one time step [*Inaoka and Takayasu*, 1993]. When the number of unstable sites remains equal to zero for a sufficiently large number of time steps, the river network is considered at its final configuration. Before reaching the equilibrium profile, the number of unstable sites remains zero, while the topography continues adjusting. The relaxation time instead is given by the time at which the topography also reaches a static steady state.

2.3. Effect of Grid Resolution

[21] We analyze the results of the numerical simulations using 256 × 256, 128 × 128 and 64 × 64 grid cells in terms of several statistics. The systems obtained at steady state with resolutions 256 × 256, 128 × 128 and 64 × 64 are
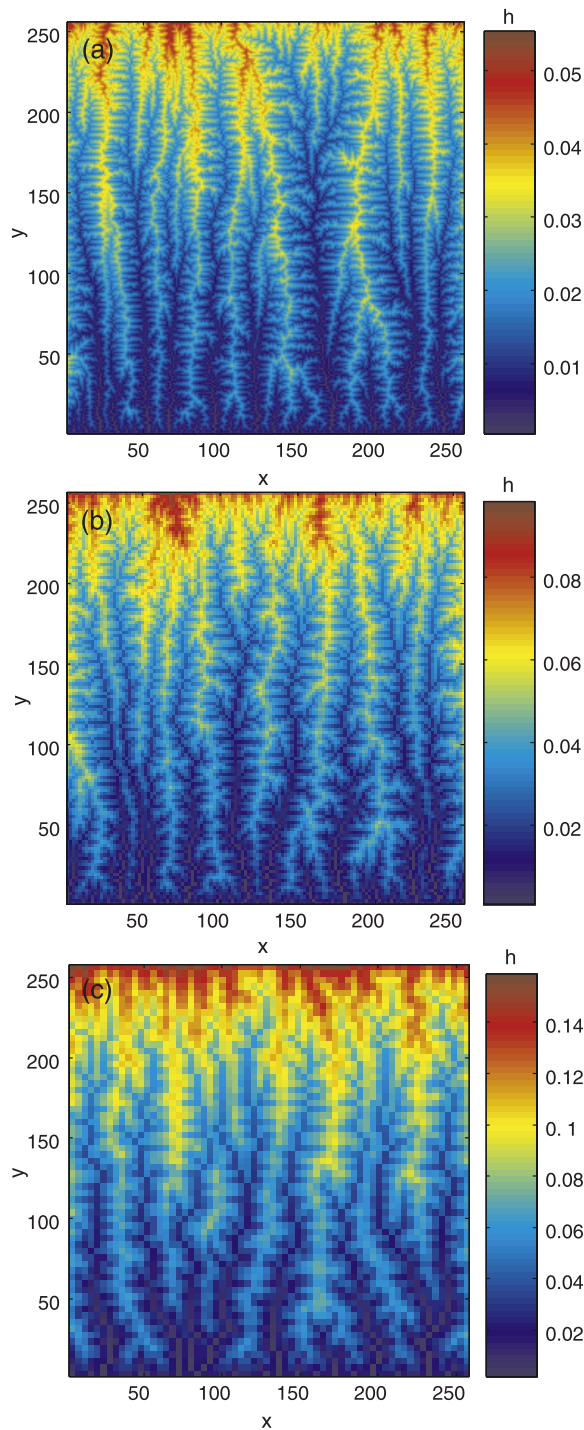
Figure 3. Elevation fields obtained for three grid resolutions at steady state using equation (5): (a) 256 × 256, (b) 128 × 128, and (c) 64 × 64.

shown in Figure 3. The corresponding river networks were extracted with River Tools (http://www.rivix.com/) and are shown in Figure 4 (channels of Strahler order greater than 2 only). The modified KPZ model produces channel networks with the expected loss of detail as the resolution is decreased.

[22] The power spectral density (spectrum) provides an estimate of the distribution of elevation variance across scales. Figure 5 shows a comparison of spectra from trans-

ects across the upstream part of the domain for the three resolutions. Except at the largest scales, there is a wide range of scales for which the spectra obtained at all resolutions show a slope of approximately −2, which is in good agreement with observations from linear transects in topography [*Vening Meinesz*, 1951; *Mandelbrot*, 1975; *Sayles and Thomas*, 1978; *Newman and Turcotte*, 1990]. However, the total variance in elevation observed at the three resolutions does depend on scale.

[23] Mean longitudinal profiles obtained at steady state with the three resolutions are shown in Figure 6a. The results indicate that the basin topography required to produce a balance between erosion and rock uplift in the simulation is strongly scale dependent. In particular, both slope and curvature increase with decreasing resolution, which is not realistic. This behavior can be attributed to the fact that erosion due to subgrid-scale channel networks (occurring at scales smaller than the grid scale) is not accounted for in the simulations. Since the subgrid-scale erosion flux is expected to be relatively larger in the case of coarser resolutions, landscapes simulated at those resolutions experience less efficient erosion than the ones obtained at higher resolutions.

[24] Strong scale dependence is also shown by the volume of material eroded per time step. As Figure 6b shows, the higher the resolution, the higher the volume of eroded material per time step. This is consistent with the observed behavior of the mean longitudinal profiles. The area under the curves, which gives the total amount of material eroded until steady state is reached, increases with resolution. The rate of erosion gives also an idea of the timescale dependence of the erosion process at the three resolutions: the higher the resolution, the higher the rate of erosion and the faster the process. The lowest resolution needs more time to reach the steady state.

3. A Dynamic Subgrid-Scale Model

3.1. Derivation of the Dynamic Subgrid-Scale Model

[25] The resolution dependence of the results obtained in the previous section using (5) highlights the need to account for the fact that erosion rates depend on the grid size used in the simulations. In this section, we develop a procedure to account for the scale dependence of the erosion coefficient α in (5). The methodology is based in part on the so-called dynamic modeling approach used in LES of turbulent flows [*Germano et al.*, 1991; *Moin et al.*, 1991; *Meneveau et al.*, 1996]. In the context of landscapes, we parameterize the effect of the subgrid-scale erosion rates by calculating a modified erosion coefficient α using information contained in the resolved elevation field and assuming scaling in the elevation statistics.

[26] For the purpose of developing the technique, one needs to know the exact value of the erosion coefficient at some reference scale. For simplicity, without loss of generality, here we consider the highest resolution simulated (256 × 256) as the exact solution, and the value of the erosion coefficient at this scale is assumed to be exactly known. However, the same approach can be extended to other reference scales for which erosion coefficients could be determined. The grid size corresponding to resolution 256 × 256 is taken as $\Delta/2$.
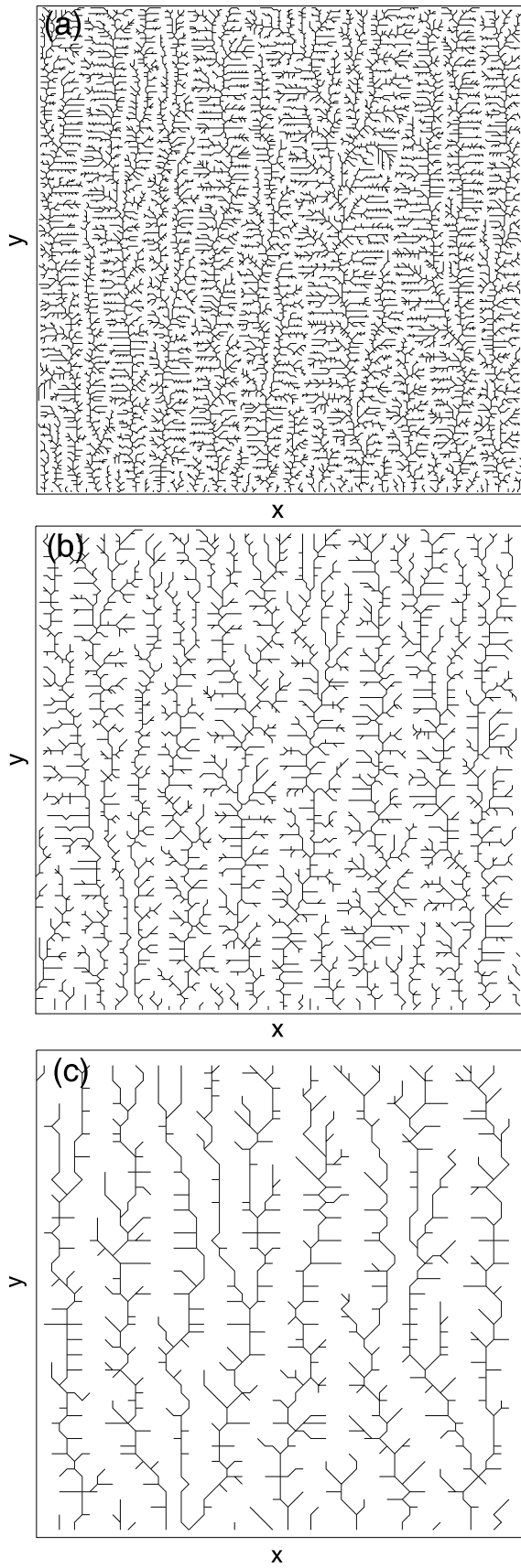
Figure 4. River network extracted from elevation fields for three grid resolutions at steady state. Only channels of Strahler order greater than 2 are shown: (a) 256×256, (b) 128×128, and (c) 64×64.

[27] At coarser resolutions the model is now written in a filtered form, as it is done in LES. At resolution 128x128 (resolution Δ), (5) becomes

$$\frac{\partial \tilde{h}}{\partial t} = u - \alpha_\Delta \cdot \tilde{q} \cdot \left| \nabla \tilde{h} \right|^2, \tag{6}$$

where the tilde indicates quantities spatially filtered (with an implicit filter imposed by the grid size) at scale Δ. At resolution 64×64 (resolution 2Δ) equation (5) becomes

$$\frac{\partial \bar{\tilde{h}}}{\partial t} = u - \alpha_{2\Delta} \cdot \bar{\tilde{q}} \cdot \left| \nabla \bar{\tilde{h}} \right|^2, \tag{7}$$

where the overbar denotes spatial filtering at scale 2Δ.

[28] Modeling erosion without explicitly accounting for scale effects on the erosion coefficient, as we did in the previous section, implicitly amounts to assuming that

$$\alpha_{2\Delta} = \alpha_\Delta = \alpha_{\Delta/2} = \alpha_0, \tag{8}$$

where α_0 is the erosion coefficient, which we assume is known and independent on resolution. The simulation results from section 2 indicate instead that α depends on the scale Δ. Our goal, then, is to account for this, dynamically computing α at each time step as the simulation progresses. To do that, one has to make some assumptions about the dependence of α on Δ. As a first approximation, we assume that the ratio between the erosion coefficients at scales Δ and $\Delta/2$ is the same as the ratio between scales 2Δ and Δ, i.e., we assume a constant value for the scale dependence ratio β, defined as

$$\beta = \frac{\alpha_\Delta}{\alpha_{\Delta/2}} \approx \frac{\alpha_{2\Delta}}{\alpha_\Delta} \approx \frac{\alpha_{4\Delta}}{\alpha_{2\Delta}}. \tag{9}$$

Note that this is a much weaker assumption than the original one that the erosion coefficient α does not depend on scale. The erosion coefficients at scales Δ (resolution
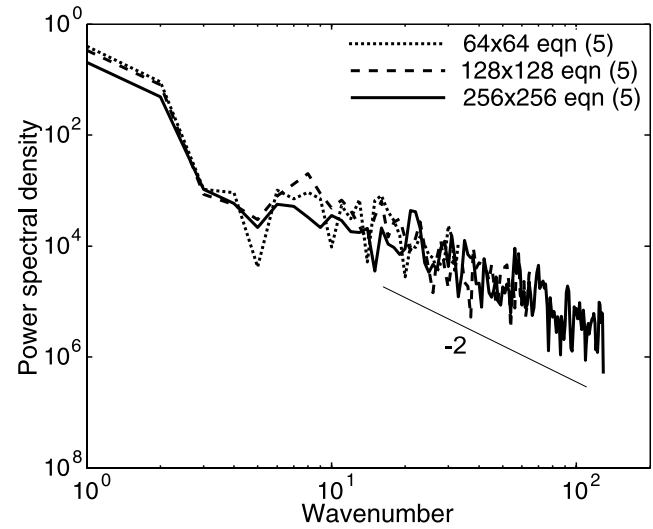

Figure 5. Elevation power spectra at the three resolutions averaged during the simulations. The spectral slope is not affected by the grid resolution and is near -2, consistent with observed spectra from natural topography.
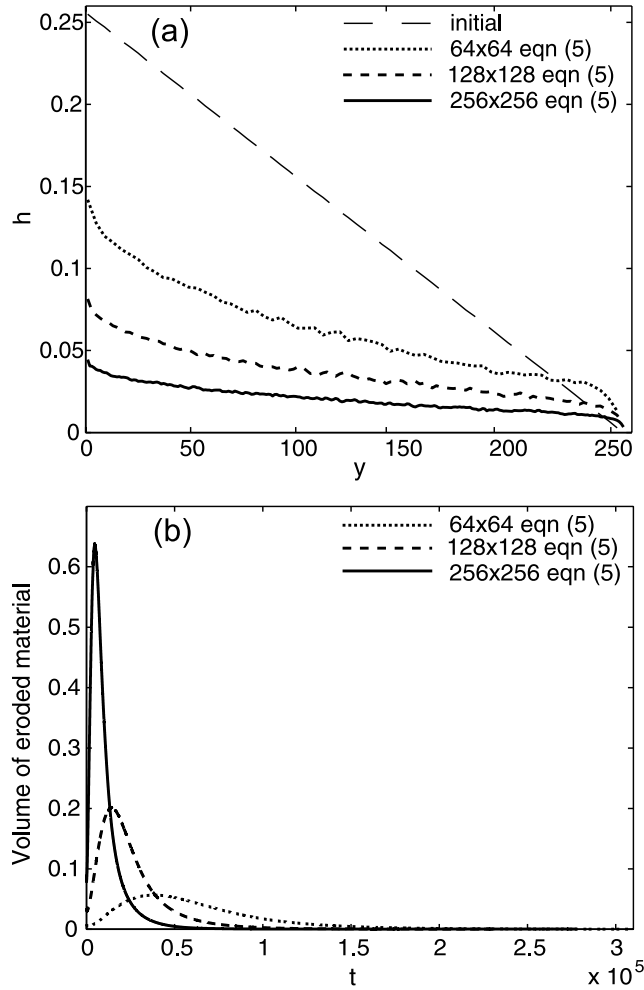
Figure 6. Dependence on grid resolution of model results using equation (5). (a) Mean longitudinal profiles obtained at steady state. (b) Volumes of eroded material per time step during the simulations. Both steady state profile and eroded volumes show strong scale dependence.

128 × 128) and 2Δ (resolution 64×64) can be expressed as a function of the erosion coefficient at the finest scale ($\Delta/2$) as follows:

$$\begin{aligned} \alpha_\Delta &= \beta \cdot \alpha_{\Delta/2} \\ \alpha_{2\Delta} &= \beta \cdot \alpha_\Delta = \beta^2 \cdot \alpha_{\Delta/2} \end{aligned} \tag{10}$$

Note that we assume the coefficient at the smallest scale equal to the known value, i.e., $\alpha_{\Delta/2} = \alpha_0$.

[29] On the basis of the expression for the scale dependence coefficient given by (9), β must be computed at scale Δ based only on information at the available scale Δ and larger, since during the simulation the behavior at finer scales is not known. Thus in our case, to compute β dynamically, we use information at scales Δ and 2Δ, together with the assumption that β is constant. The variables corresponding to scale 2Δ can easily be computed by spatially filtering the simulated field (implicitly filtered at scale Δ) using a two-dimensional filter of size 2Δ. As mentioned above, that operation is denoted by an overbar.

[30] On the basis of these ideas, we derive the new model with subgrid-scale parameterization in detail for simulations at resolution Δ. Applying the model at scales Δ and 2Δ leads to (6) and (7), given above. Spatially filtering (6) using a filter of size 2Δ (operation denoted by an overbar) and then averaging equations (6) and (7) over the entire field (operation denoted by$\langle\ \rangle$) yields

$$\left\langle \frac{\partial \bar{\bar{h}}}{\partial t} \right\rangle = \left\langle u - \alpha_\Delta \cdot \overline{\tilde{q} \cdot \left| \nabla \tilde{h} \right|^2} \right\rangle \tag{11}$$

$$\left\langle \frac{\partial \bar{\bar{h}}}{\partial t} \right\rangle = \left\langle u - \alpha_{2\Delta} \cdot \bar{\bar{q}} \cdot \left| \nabla \bar{\bar{h}} \right|^2 \right\rangle \tag{12}$$

[31] Combining (11) and (12) leads to an expression for the ratio between the effective erosion coefficients at scales 2Δ and Δ:

$$\frac{\alpha_{2\Delta}}{\alpha_\Delta} = \frac{\overline{\left\langle \tilde{q} \cdot \left| \nabla \tilde{h} \right|^2 \right\rangle}}{\left\langle \bar{\bar{q}} \cdot \left| \nabla \bar{\bar{h}} \right|^2 \right\rangle} \tag{13}$$

The right hand side of (13) can be explicitly calculated using information contained in the simulated elevation field.

[32] Taking advantage of the scale similarity assumption in (9), (13) can be used to define the scale dependence coefficient β:

$$\beta = \frac{\alpha_\Delta}{\alpha_{\Delta/2}} \approx \frac{\alpha_{2\Delta}}{\alpha_\Delta} = \frac{\overline{\left\langle \tilde{q} \cdot \left| \nabla \tilde{h} \right|^2 \right\rangle}}{\left\langle \bar{\bar{q}} \cdot \left| \nabla \bar{\bar{h}} \right|^2 \right\rangle} \tag{14}$$

Following the above procedure and using (14), we compute β dynamically at every time step, thus not requiring any a priori calibration or tuning. It is important to point out that the averaging operation ($\langle\ \rangle$) is needed to avoid unrealistic local fluctuations of β that would be obtained without averaging.

[33] The same approach can be followed to compute the coefficient β to be used in the simulations at other resolutions. For example, in the case of a grid of size 2Δ, the information at scale 4Δ would be used, and the expression for the scale dependence coefficient β would become

$$\beta = \frac{\alpha_{2\Delta}}{\alpha_\Delta} \approx \frac{\alpha_{4\Delta}}{\alpha_{2\Delta}} = \frac{\widehat{\left\langle \bar{q} \cdot \left| \nabla \bar{h} \right|^2 \right\rangle}}{\left\langle \hat{\bar{q}} \cdot \left| \nabla \hat{\bar{h}} \right|^2 \right\rangle}, \tag{15}$$

where the hat denotes a filtering operation using a two-dimensional filter of size 4Δ over the simulated variables, obtained at a grid resolution of 2Δ. Just as for scale Δ, β is computed dynamically at every time step following (15), and again does not require calibration or tuning.

[34] The new value of β is used to define the erosion coefficient $\alpha\Delta$ at the corresponding grid scale Δ in terms of
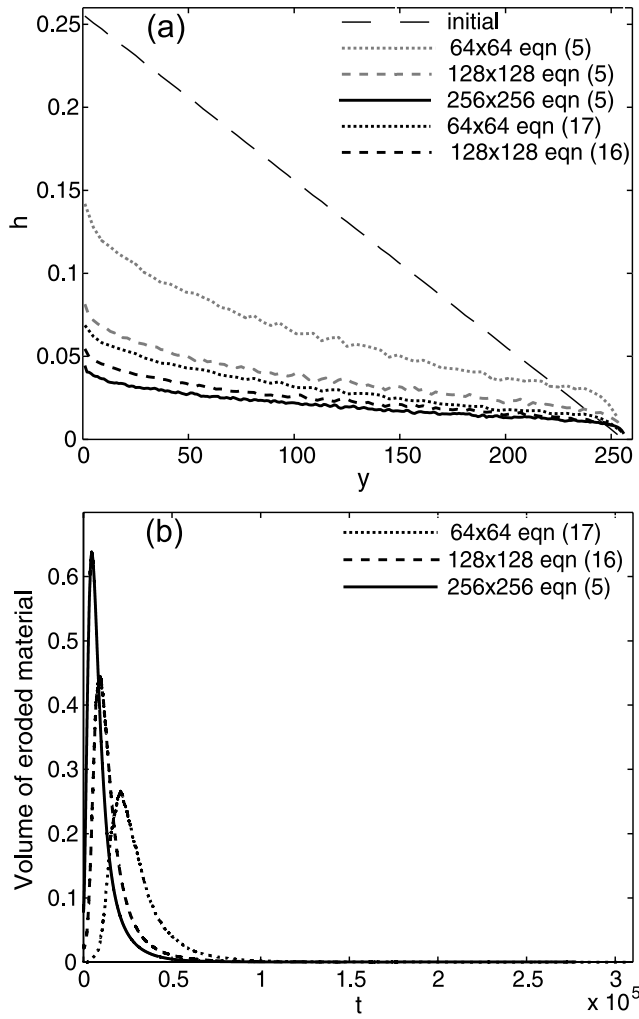
Figure 7. Comparison of results from the original model (equation (5)) and the dynamic subgrid model (equations (16) and (17)). (a) Mean longitudinal profiles obtained at steady state. The results obtained with the subgrid-scale parameterization show a relatively weak dependence on grid resolution. (b) Volumes of eroded material per time step obtained at steady state. The results obtained with the subgrid-scale parameterization again show a relatively weak dependence on grid resolution.

the erosion coefficient at scale $\Delta/2$, which we assume is exactly known, according to (10). Thus the model at scale Δ is now given by

$$\frac{\partial \tilde{h}}{\partial t} = u - \beta \cdot \alpha_{\Delta/2} \cdot \tilde{q} \cdot \left|\nabla \tilde{h}\right|^2 \qquad (16)$$

Furthermore, the model at scale 2Δ can be written as

$$\frac{\partial \bar{\tilde{h}}}{\partial t} = u - \beta^2 \cdot \alpha_{\Delta/2} \cdot \bar{\tilde{q}} \cdot \left|\nabla \bar{\tilde{h}}\right|^2 \qquad (17)$$

[35] To test the efficacy of the proposed dynamic subgrid-scale scheme, we redo the simulations at the three resolutions, using (5) at resolution 256×256, (16) at resolution 128×128 and (17) at resolution 64×64. Initial and boundary conditions are the same as used in the previous section. At every time step, the slope and the water flux are

computed at each location from the simulated field. Then the field is filtered at a resolution double the grid size and slope and water flux are computed from the filtered field at each location. With these quantities the scale dependence coefficient β is computed from equation (14) (or (15) at 64×64) and the field is then updated using equation (16) (or (17) at 64×64).

3.2. Results and Discussion

[36] The elevation fields and the extracted river networks are qualitatively similar to the ones obtained in the previous section using equation (5) at all resolutions. However, the erosion rate is clearly affected by the new formulation of the model at the lower resolutions. The mean longitudinal profiles obtained at steady state for the simulations with dynamic subgrid-scale modeling are shown in Figure 7a. The profiles at resolution 128×128 and 64×64 obtained with the new model are close to the profile at 256×256, indicating that the dynamic subgrid-scale method accounts for most of the scale dependence. The same behavior is found in the volume of eroded material per time step, shown in Figure 7b: the new model with dynamic subgrid-scale parameterization yields much more consistent erosion rates across the different grid resolutions than the simulations using a constant erosion coefficient.

[37] We stress that in this first stage of our investigation, we have used the simplest plausible scheme for dynamic subgrid-scale modeling. Despite this, the method seems able to eliminate much of the dependence of erosional landscape dynamics on grid resolution. The dynamic procedure is now modified to allow for scale dependence of the coefficient β. A similar dynamic, tuning-free approach has recently been developed in the context of subgrid-scale models for LES of turbulent flows [*Porté-Agel et al.*, 2000; *Porté-Agel*, 2004; *Stoll and Porté-Agel*, 2006.].

4. A Scale-Dependent Dynamic Subgrid-Scale Model

4.1. Derivation of the Scale-Dependent Dynamic Subgrid-Scale Model

[38] The dynamic procedure is now modified to allow for scale dependence of the coefficient β. This requires the use of an additional test filtering operation (e.g., at scale four times the grid scale), from which the scale dependence of β can be determined dynamically. The scale dependence coefficient β is now allowed to change with scale, and therefore

$$\beta_\Delta \neq \beta_{2\Delta} \neq \beta_{4\Delta}. \qquad (18)$$

[39] At this point, an assumption has to be made about the functional form of the scale dependence of β. Assuming a simple power law dependence of β with scale [*Porté-Agel et al.*, 2000], we can write

$$\frac{\beta_\Delta}{\beta_{2\Delta}} \approx \frac{\beta_{2\Delta}}{\beta_{4\Delta}} \approx \frac{\beta_{4\Delta}}{\beta_{8\Delta}}. \qquad (19)$$

Note that this is a much weaker assumption than the previous one of β constant across scales. Using equation (19), the
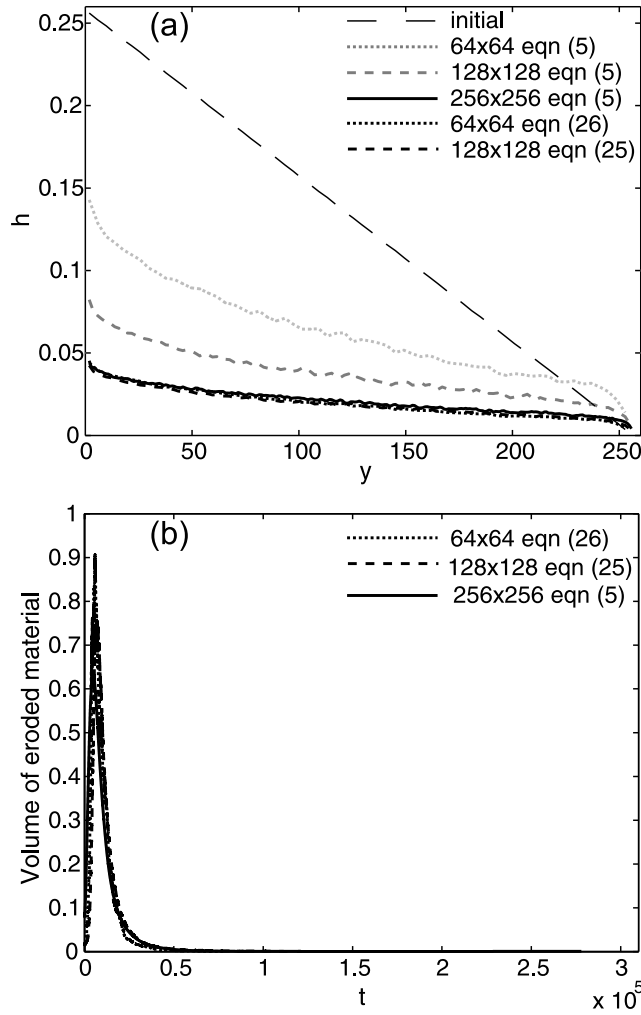
Figure 8. Comparison of the results from the original model (equation (5)) and the new scale-dependent dynamic subgrid model (equations (25) and (26)). (a) Mean longitudinal profiles obtained at steady state. The profiles obtained with the subgrid-scale parameterization are almost indistinguishable. (b) Volumes of eroded material per time step obtained at steady state. The results obtained with the subgrid-scale parameterization again show very little dependence on grid resolution and time.

scale dependence coefficient at scale Δ, β_Δ, can be expressed as

$$\beta_\Delta \approx \beta_{2\Delta} \cdot \frac{\beta_{2\Delta}}{\beta_{4\Delta}} = \frac{\beta_{2\Delta}^2}{\beta_{4\Delta}}, \tag{20}$$

where $\beta_{2\Delta}$ and $\beta_{4\Delta}$, recalling (14) and (15), can be computed dynamically from the resolved elevation field as

$$\beta_{2\Delta} = \frac{\alpha_{2\Delta}}{\alpha_\Delta} = \frac{\left\langle \widetilde{\tilde{q} \cdot |\nabla \tilde{h}|^2} \right\rangle}{\left\langle \widetilde{\bar{\tilde{q}} \cdot |\nabla \bar{\tilde{h}}|^2} \right\rangle}$$

$$\tag{21}$$

$$\beta_{4\Delta} = \frac{\alpha_{4\Delta}}{\alpha_{2\Delta}} = \frac{\left\langle \widetilde{\bar{q} \cdot |\nabla \bar{h}|^2} \right\rangle}{\left\langle \widetilde{\hat{q} \cdot |\nabla \hat{h}|^2} \right\rangle},$$

The same procedure can be applied at scale 2Δ to express the unknown parameters β_Δ and $\beta_{2\Delta}$ as a function of $\beta_{4\Delta}$ and $\beta_{8\Delta}$ as

$$\beta_{2\Delta} \approx \beta_{4\Delta} \cdot \frac{\beta_{4\Delta}}{\beta_{8\Delta}},$$

$$\beta_\Delta \approx \beta_{2\Delta} \cdot \frac{\beta_{2\Delta}}{\beta_{4\Delta}} = \left(\beta_{4\Delta} \cdot \frac{\beta_{4\Delta}}{\beta_{8\Delta}} \right)^2 \cdot \frac{1}{\beta_{4\Delta}} = \frac{\beta_{4\Delta}^3}{\beta_{8\Delta}^2}, \text{ and} \tag{22}$$

$$\beta_{2\Delta} \cdot \beta_\Delta \approx \frac{\beta_{4\Delta}^5}{\beta_{8\Delta}^3}$$

Note that $\beta_{4\Delta}$ can be obtained from the resolved elevation field using equation (21), and $\beta_{8\Delta}$ can also be computed dynamically using the identity

$$\beta_{8\Delta} = \frac{\alpha_{8\Delta}}{\alpha_{4\Delta}} = \frac{\left\langle \widehat{\hat{q} \cdot |\nabla \hat{h}|^2} \right\rangle}{\left\langle \widehat{\hat{q} \cdot |\nabla \hat{h}|^2} \right\rangle}, \tag{23}$$

where the curved overbar denotes a filtering operation using a two-dimensional filter of size 8Δ over the simulated variables, obtained at a grid resolution of 2Δ.

[40] With the new definitions of β_Δ and $\beta_{2\Delta}$, α_Δ and $\alpha_{2\Delta}$ become

$$\alpha_\Delta = \beta_\Delta \cdot \alpha_{\Delta/2} = \frac{\beta_{2\Delta}^2}{\beta_{4\Delta}} \cdot \alpha_{\Delta/2}$$

$$\tag{24}$$

$$\alpha_{2\Delta} = \beta_{2\Delta} \cdot \beta_\Delta \cdot \alpha_{\Delta/2} = \frac{\beta_{4\Delta}^5}{\beta_{8\Delta}^3} \cdot \alpha_{\Delta/2}$$

and equations (16) and (17) become

$$\frac{\partial \tilde{h}}{\partial t} = u - \frac{\beta_{2\Delta}^2}{\beta_{4\Delta}} \cdot \alpha_{\Delta/2} \cdot \tilde{q} \cdot |\nabla \tilde{h}|^2 \tag{25}$$

$$\frac{\partial \bar{\tilde{h}}}{\partial t} = u - \frac{\beta_{4\Delta}^5}{\beta_{8\Delta}^3} \cdot \alpha_{\Delta/2} \cdot \bar{\tilde{q}} \cdot |\nabla \bar{\tilde{h}}|^2 \tag{26}$$

To test the proposed scale-dependent dynamic subgrid-scale scheme, we perform the same simulations using equation (5) at resolution 256×256, and equations (25) and (26) at resolutions 128×128 and 64×64, respectively.

[41] Initial and boundary conditions are the same used in the previous sections. At every time step, the slope and the water flux are computed at each location from the simulated field. Then the field is filtered at a resolution two and four times the grid size and slope and water flux are computed from the filtered field at each location. The scale dependence coefficients β corresponding to scales twice and four times the grid scale are computed dynamically using equations (21) for the 128×128 resolution, or equations (21) and (23) for the 64×64 resolution. These values are then used in equations (25) and (26) to obtain the time evolution of the simulated elevation field. The simulations are run until steady state is reached.

4.2. Results and Discussion

[42] Similar to the case of the dynamic model presented in Section 3, the elevation fields and river networks obtained with the scale-dependent dynamic model are

quantitatively similar to the ones obtained without subgrid-scale model. However, the mean longitudinal profile obtained at steady state and the volume of eroded material per time step show an additional improvement compared to the scale-invariant dynamic model. As shown in Figures 8a and 8b, the simulation results obtained with the three resolutions are very similar, which highlights the ability of the new model to systematically (and without parameter tuning) account for the scale dependence of the erosion coefficient. Moreover, the previously observed time dependence of the results is substantially reduced (Figure 8b), indicating that the new model is also able to minimize the effects of resolution on the time evolution of the simulated landscapes.

[43] Note that there are a number of ways in which the scale-dependent dynamic approach could be improved. For example, the coefficient β could be computed locally using alternative averaging methods, such as the Lagrangian dynamic procedure introduced by *Meneveau et al.* [1996]. High-resolution digital elevation data could also be used to test some of the assumptions made in the dynamic models (e.g., power law scaling of the coefficients) and provide guidance for further improvements, as done in a priori experimental studies of turbulent flows [e.g., *Meneveau and Katz*, 2000].

5. Conclusions

[44] 1. Landscapes simulated using a modified 2-D KPZ equation show a systematic dependence on grid resolution: increasing resolution allows for increased channel density, and thus erosion rates and mean longitudinal profiles of elevation at steady state have an undesirable dependence on grid resolution.

[45] 2. A new subgrid-scale parameterization, inspired by the scale-dependent dynamic modeling approach used in turbulence simulations, is able to correct most of this scale dependence. The erosion coefficient, assumed exactly known at the finest resolution, is multiplied by a scale dependence coefficient, which is computed dynamically as a function of time based on the landscape dynamics at the resolved scales. The scheme takes advantage of the self-similarity that characterizes landscapes over a wide range of scales and produces landscapes that show very little dependence on grid resolution.

[46] There is no reason the proposed approach could not be applied to other landscape evolution models. The applicability of the LES-inspired approach to modeling erosional landscapes suggests that the technique may be generalizable to other systems as well. The basic requirement is that the system be self-similar over a sufficiently wide range of length scales to justify the estimation of the effect of subgrid processes by comparison of the model behavior over scales coarser than the resolved scale. Possible candidates in morphodynamics include braided rivers [*Sapozhnikov and Foufoula-Georgiou*, 1996, 1997], distributary channel networks, and bed forms.

References

Adams, J. (1980), Contemporary uplift and erosion of Southern Alps, New Zealand: Summary, *Geol. Soc. Am. Bull.*, *91*, 2–4.

Banavar, J., F. Colaiori, A. Flammini, A. Maritan, and S. Rinaldo (2001), Scaling, optimality and landscape evolution, *J. Stat. Phys.*, *104*, 1–49.

Bear, I. (1988), *Dynamics of Fluids in Porous Media*, 784 pp., Dover, Mineola, N. Y.

Bou-Zeid, E., C. Meneveau, and M. B. Parlange (2004), Large-eddy simulation of neutral atmospheric boundary layer flow over heterogeneous surfaces: Blending height and effective surface roughness, *Water Resour. Res.*, *40*, W02505, doi:10.1029/2003WR002475.

Chase, C. G. (1992), Fluvial landsculpting and the fractal dimension of topography, *Geomorphology*, *5*, 39–57.

Culling, W. E. H. (1960), Analytical theory of erosion, *J. Geol.*, *68*, 336–344.

Culling, W. E. H. (1963), Soil creep and the development of hillside slopes, *J. Geol.*, *71*, 127–161.

Dietrich, W. E., D. Bellugi, A. M. Heimsath, J. J. Roering, L. Sklar, and J. D. Stock (2003), Geomorphic transport laws for predicting landscape form and dynamics, in *Prediction in Geomorphology*, *Geophys. Monogr. Ser.*, vol. 136 edited by P. Wilcock and R. Iverson, pp. 103-132, AGU, Washington, D. C.

Germano, M., U. Piomelli, P. Moin, and W. H. Cabot (1991), A dynamic subgrid-scale eddy viscosity model, *Phys. Fluids*, *3*, 1760–1765.

Geurts, B. J. (2004), *Elements of Direct and Large Eddy Simulations*, 388 pp., R. T. Edwards, Flourtown, Pa.

Hack, J. T. (1960), Interpretation of erosional topography in humid temperate regions, *Am. J. Sci.*, *258A*, 80–97.

Harris, D., and E. Foufoula-Georgiou (2001), Subgrid variability and stochastic downscaling of modeled clouds: Effects on radiative transfer computations for rainfall retrieval, *J. Geophys. Res.*, *106*, 10,349–10,362.

Hasbargen, L. E., and C. Paola (2000), Landscape instability in an experimental drainage basin, *Geology*, *28*, 1067–1070.

Hasbargen, L., and C. Paola (2003), How predictable is local erosion rate in erosional landscapes?, in *Prediction in Geomorphology*, *Geophys. Monogr. Ser.*, vol. *136* edited by P. R. Wilcock and R. M. Iverson, pp. 231–240, AGU, Washington, D. C.

Howard, A. D. (1994), A detachment-limited model of drainage basin evolution, *Water Resour. Res.*, *30*, 2261–2285.

Inaoka, H., and H. Takayasu (1993), Water erosion as a fractal growth process, *Phys. Rev. E*, *47*, 899–910.

Kagan, Y. Y. (1992), Seismicity: The turbulence of solids, *Nonlinear Sci. Today*, *2*, 123–134.

Kardar, M., G. Parisi, and Y.-C. Zhang (1986), Dynamic scaling of growing interfaces, *Phys. Rev. Lett.*, *56*, 889–892.

Kolmogorov, A. (1961), Dissipation of energy in the locally isotropic turbulence, in *Turbulence: Classic Papers on Statistical Theory*, edited by S. K. Friedlander and L. Topper, pp. 151–155, Wiley-Interscience, Hoboken, N. J.

Kooi, H., and C. Beaumont (1994), Escarpment evolution on high-elevation rifted margins: Insights derived from a surface-processes model that combines diffusion, advection, and reaction, *J. Geophys. Res.*, *99*, 12,191–12,209.

Koons, P. O. (1995), Modelling the topographic evolution of collisional mountain belts, *Annu. Rev. Earth Planet. Sci.*, *23*, 375–408.

Mandelbrot, B. (1975), Stochastic models for the Earth's relief, the shape and the fractal dimension of coastlines, and the number-area rule for islands, *Proc. Natl. Acad. Sci. U.S.A.*, *72*, 3825–3828.

Meneveau, C., and J. Katz (2000), Scale invariance and turbulence models for large-eddy simulation, *Annu. Rev. Fluid Mech.*, *32*, 1–32.

Meneveau, C., T. S. Lund, and W. H. Cabot (1996), A Lagrangian dynamic subgrid-scale model of turbulence, *J. Fluid Mech.*, *319*, 353–385.

Moin, P., K. D. Squires, and S. Lee (1991), A dynamic subgrid-scale model for compressible turbulence and scalar transport, *Phys. Fluids*, *3*, 2746–2757.

Newman, W. I., and D. L. Turcotte (1990), Cascade model for fluvial geomorphology, *Geophys. J. Int.*, *100*, 433–439.

Paola, C. (1996), Incoherent structure: Turbulence as a metaphor for stream braiding, in *Coherent Flow Structures in Open Channels*, edited by P. J. Ashworth et al., pp. 705–723, John Wiley, Hoboken, N. J.

Paola, C., G. Parker, D. C. Mohrig, and K. X. Whipple (1999), The influence of transport fluctuations on spatially averaged topography on a sandy, braided fluvial fan, in *Numerical Experiments in Stratigraphy: Recent Advances in Stratigraphic and Sedimentologic Computer Simulations*, edited by J. Harbaugh et al., *Spec. Publ. SEPM Soc. Sediment. Geol.*, *62*, 211–218.

Peckham, S. D. (1995), Self-similarity in the three-dimensional geometry and dynamics of large river basins, Ph.D. thesis, Univ. of Colo., Boulder.

Peckham, S. D. (2003), Fluvial landscape models and catchment-scale sediment transport, *Global Planet. Change*, *39*, 31–51.

Pelletier, J. D. (2004), Persistent drainage migration in a numerical land-form evolution model, *Geophys. Res. Lett.*, 31, L20501, doi:10.1029/2004GL020802.

Pope, S. B. (2000), *Turbulent Flows*, 771 pp., Cambridge Univ. Press, New York.

Pope, S. B. (2004), Ten questions concerning the large-eddy simulation of turbulent flows, *New J. Phys.*, 6, 35.

Porté-Agel, F. (2004), A scale-dependent dynamic model for scalar trans-port in the atmospheric boundary layer, *Boundary Layer Meteorol.*, 112, 81–105.

Porté-Agel, F., C. Meneveau, and M. B. Parlange (2000), A scale-dependent dynamic model for large-eddy simulation: Application to a neutral atmospheric boundary layer, *J. Fluid Mech.*, 415, 261–284.

Rinaldo, A., I. Rodriguez-Iturbe, R. Rigon, R. L. Bras, E. Ijjasz-Vasquez, and A. Marani (1992), Minimum energy and fractal structures of drai-nage networks, *Water Resour. Res.*, 28, 2183–2195.

Rodriguez-Iturbe, I., and A. Rinaldo (1997), *Fractal River Basins*, 539 pp., Cambridge Univ. Press, New York.

Rodriguez-Iturbe, I., M. Marani, R. Rigon, and A. Rinaldo (1994), Self-organized river basin landscapes: Fractal and multifractal characteristics, *Water Resour. Res.*, 30, 3531–3539.

Sagaut, P. (2002), *Large Eddy Simulation for Incompressible Flows: An Introduction*, 426 pp., Springer, New York.

Sapozhnikov, V. B., and E. Foufoula-Georgiou (1996), Self-affinity in braided rivers, *Water Resour. Res.*, 32, 1429–1439.

Sapozhnikov, V. B., and E. Foufoula-Georgiou (1997), Experimental evi-dence of dynamic scaling and indications of self-organized criticality in braided rivers, *Water Resour. Res.*, 33, 1983–1991.

Sayles, R. S., and T. R. Thomas (1978), Surface topography as a non-stationary random process, *Nature*, 271, 431–434.

Sinclair, K., and R. C. Ball (1996), Mechanism for global optimization of river networks from local erosion rules, *Phys. Rev. Lett.*, 76, 3360–3363.

Smith, T. R., G. E. Merchant, and B. Birnir (1997a), Towards an elementary theory of drainage basin evolution: I. The theoretical basis, *Comput. Geosci.*, 23(8), 811–822.

Smith, T. R., G. E. Merchant, and B. Birnir (1997b), Towards an elementary theory of drainage basin evolution: II. A computational evaluation, *Comput. Geosci.*, 23(8), 823–849.

Somfai, E., and L. M. Sander (1997), Scaling and river networks—A Land-au theory for erosion, *Phys. Rev. E*, 56, R5–R8.

Sornette, D., and Y.-C. Zhang (1993), Non linear Langevin model of geo-morphic erosion processes, *Geophys. J. Int.*, 113, 382–386.

Stark, C. P., and G. J. Stark (2001), A channelization model of landscape evolution, *Am. J. Sci.*, 301, 486–512.

Stoll, R., and F. Porté-Agel (2006), Dynamic subgrid-scale models for momentum and scalar fluxes in large-eddy simulations of atmospheric boundary layers over heterogeneous terrain, *Water Resour. Res.*, 42, W01409, doi:10.1029/2005WR003989.

Tucker, G. E., and R. L. Slingerland (1994), Erosional dynamics, flexural isostasy, and long-lived escarpments: A numerical modeling study, *J. Geophys. Res.*, 99, 12,229–12,243.

Tucker, G. E., S. T. Lancaster, N. M. Gasparini, and R. L. Bras (2001), The channel-hillslope integrated landscape development (CHILD) model, in *Landscape Erosion and Evolution Modeling*, edited by R. S. Harmon and W. W. Doe III, pp. 349–388, Springer, New York.

Vening Meinesz, F. A. (1951), A remarkable feature of the Earth's topo-graphy, *Proc. K. Ned. Akad. Wet. Ser. B. Palaeontol. Geol Phys. Chem. Anthropol.*, 54, 212–228.

Willett, S. D., and M. T. Brandon (2002), On steady states in mountain belts, *Geology*, 30, 175–178.

Willgoose, G. (2005), Mathematical modeling of whole landscape evolu-tion, *Annu. Rev. Earth Planet. Sci.*, 33, 443–459.

Willgoose, G., R. L. Bras, and I. Rodriguez-Iturbe (1991a), A coupled channel network growth and hillslope evolution model: 2. Nondimensio-nalization and applications, *Water Resour. Res.*, 27, 1685–1696.

Willgoose, G., R. L. Bras, and I. Rodriguez-Iturbe (1991b), A coupled channel network growth and hillslope evolution model: 1. Theory, *Water Resour. Res.*, 27, 1671–1684.

————————————

E. Foufoula-Georgiou, C. Paola, F. Porté-Agel, and P. Passalacqua, St. Anthony Falls Laboratory, 2 Third Avenue SE, Minneapolis, MN 55414, USA. (cpaola@umn.edu)